2014 IEEE International Conference on Robotics & Automation (ICRA)
Hong Kong Convention and Exhibition Center
May 31 - June 7, 2014. Hong Kong, China

Posture Control of a Three-Segmented Tracked Robot with Torque Minimization During Step Climbing

Sartaj Singh[1], Babu D Jadhav[1] and K Madhava Krishna[2]

Abstract— **In this paper, we present a posture control scheme for step climbing by an in-house developed three-segmented tracked robot, miniUGV. The posture control scheme results in minimum torque at the actuated joints of the segments. Non-linear optimization is carried out offline for progressively decreasing distance of the robot from the step with torque minimization as objective function and force balance, motor torque limits, slippage avoidance and interference avoidance constraints. The resulting angles of the joints are fitted to a third degree polynomial as a function of the robot distance from the step and the step height. It is shown that a single set of polynomial functions is sufficient for climbing steps of all permissible heights and angles of attack of the front segment. The methodology has been verified through simulation followed by implementation on the real robot. As a consequence of this optimization we find that the average current reduced by more than thirty percent, reducing power consumption and confirming the efficacy of the optimization framework.**

I. INTRODUCTION

Energy optimization in step climbing by tracked mobile robots is the focus of this paper. Miniature mobile robots are often used in urban and off-road scenarios where steps are a common feature of the terrain. Tracked locomotion is highly suitable for such terrain and various configurations of tracked robots have been developed and are available commercially. Examples of these are the fixed track robots, e.g. Talon [1] and Matilda [2], tracks with flippers robots, e.g. Packbot [3] and dual flipper robots, e.g. Chaos [4]. We have developed a man-portable three segmented tracked robot called miniUGV. This robot has been developed with the aim of carrying out surveillance in urban and off-road scenarios. The robot is often required to cross stepped structures such as foot-paths, ledges, thresholds, railway tracks and piles of debris or construction material, wherein the robot needs to traverse over several vertical discontinuities. In [5] and [6] design of single segment tracked robots suitable for step/stair climbing has been carried out. Multi-segmented and variable geometry based tracked robots can make use of their re-configurability to climb steps higher than the diameter of drive pulleys. However making these robots climb purely by teleoperation is a difficult task. Hence autonomous techniques for climbing steps/stair with minimal sensors and computational requirement need to be devised. In [7], [8], [9] and [10] force analysis and interference avoiding criteria has been used to determine the feasible postures at various stages of climbing which result in stable configurations. In [11] on-board camera is used to determine the state of the robot with respect to stairs for autonomous stable climbing. In [12] computer vision along with inertial sensors is used for determining parameters of stairs and state of the robot for stable climbing. All the research effort in these systems focuses on arriving at kinematically feasible and stable states of robot for climbing steps/stairs.

However energy consumption is also a critical factor to be taken into account during step/stair climbing. Mobile robots require lesser power for traversing on flat terrain as compared to climbing steps or stairs. Reconfigurable robots can be made to adopt postures during step climbing which result in less power consumption. Control schemes for energy optimization have been developed for wheeled robots with passive and active suspension mechanisms [13], [14] and [15]. However, the energy optimization in these systems focused on minimizing the traction forces at the wheel ground interaction rather than torques of active joints. No similar schemes for multi-segmented tracked robots have been reported in the literature.

A major difference between wheeled and tracked robots is the location of contact point between robot and terrain. The contact points in wheeled robots are limited to the circumference of the wheel while the contact point on tracked robots can move over full length of the track. Additionally, location of the contact point depends on the approach angle of the tracks. Hence a methodology needs to be developed that take into account the shifting contact point.

In this paper we present a methodology to determine the posture of the three-segmented tracked robot, miniUGV, during step climbing which results in torque minimization. The resulting posture has been implemented using two third degree polynomials which are a function of the step distance and height of the step. At present, the robot has no sensors for measuring step height and step distance. Step height is fed a priori to the robot and the robot velocity is used to estimate the step distance. However, step height and distance can easily be measured by integration of a laser range scanner. The polynomial curves used for posture control generalize step climbing over various heights and approach angle of the robot. The maximum step height traversable with scheme presented is 0.325m and results in reduction of power consumption by nearly 30%. The methodology has been verified by multi-body dynamics simulation tool, MSC VISUAL NASTRAN and implemented on the three-segmented robot, miniUGV.

[1]Sartaj Singh and Babu D Jadhav are with Centre for AI and Robotics (CAIR), DRDO, India. sartajsinghishar@gmail.com, babu.damla@gmail.com

[2]Dr. K Madhava Krishna is with Robotics Research Centre, IIIT-Hyderabad, India. mkrishna@iiit.ac.in

II. NOVELTIES

A key advantage of the methodology presented in this work is that the posture control scheme can be implemented in real time with minimal computational overhead. Posture control is achieved using single set of polynomials for calculating the desired angles of the segments as a function of step distance and step height. A single set of polynomials that generalizes over various step heights and angle of attacks of the robot does not seem to have been reported in earlier literature. Apart from computational savings the optimization framework results in significantly lower power budget that is crucial in several outdoor scenarios where the robot has to traverse terrain with limited onboard batteries. This scheme helps to determine the instantaneous postures which result in minimum torque requirement to maintain a statically stable state. Hence the power consumption is reduced irresapective of the speed of the robot resulting in overall energy minimization.

III. SYSTEM DESCRIPTION

Fig. 1 shows the three-segmented robot, miniUGV. The three segments comprise the rear, front and middle segments connected through active joints. Each of these segments has two tracked sections placed symmetrically about the central longitudinal plane. Sections to the right constitute the right-track while to the left constitute the left-track. The rear and front segments and the right and left tracks are driven independently by PMDC servomotors. Middle segment is a fixed height section while front and rear segments are tapered. The middle segment has been slightly raised in the real robot to accommodate the electronics. However a symmetric shape has been used for analysis as this has no effect on the optimization.

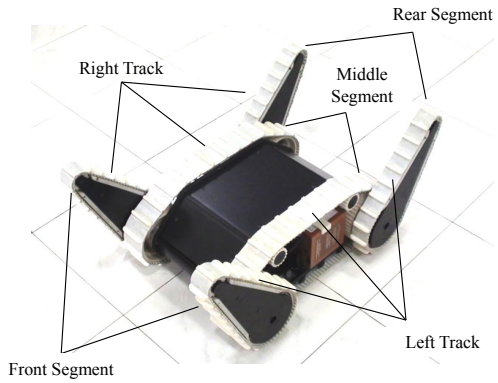

Fig. 1. Actual prototype of the three-segmented miniUGV robot

Fig. 2 shows the front and top views of the CAD model of miniUGV. Important parameters of miniUGV used for analysis are listed in Table I.

A distributed controller has been developed for miniUGV for speed control of the track motors and position control of the joint motors. Each motor controller has a dedicated microcontroller which communicates with a master controller using CAN bus. The master controller receives high level commands from a PC104 Linux box. The Linux box communicates with a hand-held operator control unit or host computer using a dedicated wireless link. The Linux box is also used for capturing, compressing and sending the data from two onboard cameras.

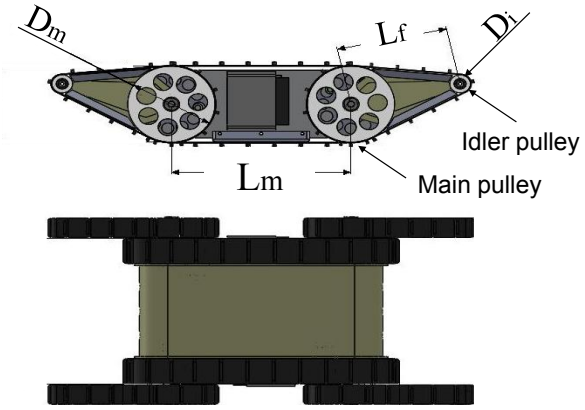

Fig. 2. Front and top views of miniUGV CAD model

TABLE I
MINIUGV PARAMETERS

Parameter	Value
Length of middle segment, L_m	0.40 m
Length of front and rear segment, L_f	0.28 m
Diameter of main pulley, D_m	0.175 m
Diameter of idler pulley, D_i	0.05 m
Mass of main segment, M_m	22 kg
Mass of front (rear) segment,M_f	4 kg
Maximum Torque of right (left) track motor, $\tau_t max$	5 Nm
Maximum Torque of front (rear) joint motor,$\tau_j max$	35 Nm

Step climbing sequence for miniUGV is shown in Fig. 3. The sequence has three distinct stages. In nominal state, the front segment is at an angle called angle of attack and rear segment is horizontal. Stage-1 of climbing starts as soon as the front segment comes in contact with the step edge and continues till the front segment crosses the step edge. Stage-2 starts at this point and continues till the centre of mass (CoM) of middle segment has crossed the step edge. Stages-3 starts at this point and continues till the whole robot has crossed the step.

IV. PROBLEM DEFINITION

Amongst the three stages of climbing, stage-1 and stage-2 are the most power consuming stages. In these stages the entire mass of the robot gets lifted. In stage-3 the balancing moment topples the whole body towards the front. As a result the robot is fully supported by middle segment and no load comes on the joints of front and rear segments. We therefore analyzed stage-1 and stage-2 of climbing for energy minimization. However, the energy minimum posture throughout the stage-2 is same as the last optimized posture in stage-1. Hence analysis was carried out for stage-1 of climbing. Energy consumed depends on the current drawn by the motors which in turn determine the torque required for maintaining a

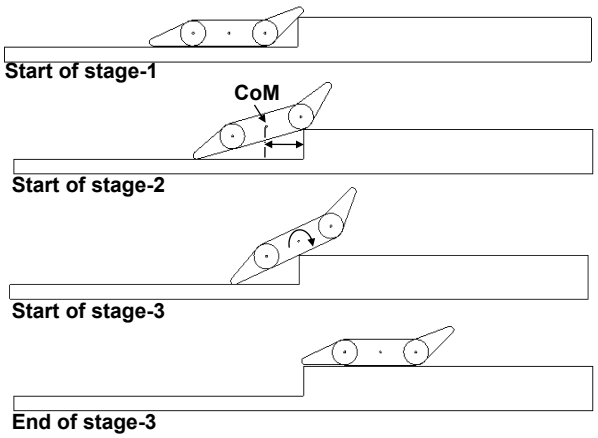

Fig. 3. Three stages of step climbing sequence

particular posture. Hence the energy minimization is carried out as a posture control optimization problem with torque minimization as objective function. We seek to determine the angles of front and rear segments using the optimization which fully define the posture of the robot. To carry out the optimization, system constraints need to be defined which result in a feasible solution. The system constraints can be divided into force balance, torque limit, slippage avoidance, geometric and interference avoidance constraints. Analysis for determining the constraints is carried out for planar case since the robot is symmetric about the central longitudinal plane.

A. Force Balance Constraint

The force balance equations which satisfy static equilibrium for the stage-1 are determined using the free body diagram (FBD) shown in Fig. 4.

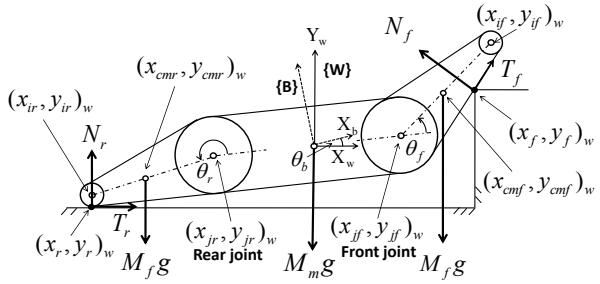

Fig. 4. Free Body Diagram of stage-1 of climbing

The robot has two coordinate frames; one is body frame B which is fixed at CoM of middle segment with X-axis pointing towards front and second is world frame W with origin same as B but having Y-axis aligned to gravity. Hence B can have rotation with respect to W equal to pitch, θ_b, of the middle segment. Angles of the front and rear segments with respect to the middle segment are θ_f and θ_r respectively. In stage-1 the robot has two contact points with the terrain: front contact point between the front segment and step corner with coordinates $(x_f, y_f)_W$ and rear contact point between rear segment and ground with coordinates $(x_r, y_r)_W$. The normal reaction and tractive forces at the contact points are N_f, T_f,N_r and T_r. Description of the symbols used for analyzing the FBD is given in Table II.

TABLE II
DESCRIPTION OF SYMBOLS USED IN ANALYSIS

B	Body Frame
W	World Frame
N_f	Normal reaction at front contact point
T_f	Tractive force at front contact point
N_r	Normal reaction at rear contact point
T_r	Tractive force at rear contact point
$(x_f, y_f)_W$	Coordinates of front contact point in W
$(x_r, y_r)_W$	Coordinates of rear contact point
$(x_{jf}, y_{jf})_W$	Coordinates of front segment joint
$(x_{jr}, y_{jr})_W$	Coordinates of rear segment joint
$(x_{cmf}, y_{cmf})_W$	Coordinates of front segment CoM
$(x_{cmr}, y_{cmr})_W$	Coordinates of rear segment CoM
$(x_{if}, y_{if})_W$	Coordinates of front segment idler pulley
$(x_{ir}, y_{ir})_W$	Coordinates of rear segment idler pulley
θ_b	Pitch angle of body
θ_f	angle of front segment in B
θ_r	angle of rear segment in B

The force/moment balance equations for FBD are given by (1), (2) and (3).

$$F_x = T_r + T_f cos(\theta_b + \theta_f) - N_f sin(\theta_b + \theta_f) \quad (1)$$

$$F_y = N_r - M_f g - M_m g - M_f g + N_f cos(\theta_b + \theta_f) + T_f sin(\theta_b + \theta_f) \quad (2)$$

$$\begin{aligned} M_z = {} & N_f cos(\theta_b + \theta_f)(x_f - x_r) \\ & + N_f sin(\theta_b + \theta_f)(y_f - y_r) \\ & - T_f cos(\theta_b + \theta_f)(y_f - y_r) \\ & + T_f sin(\theta_b + \theta_f)(x_f - x_r) \\ & - M_f g(x_{cmf} - x_r) - M_m g(-x_r) \\ & - M_f g(x_{cmr} - x_r) \end{aligned} \quad (3)$$

B. Torque limit constraint

The front and rear segment joint motor torques are given by (4) and (5)

$$\tau_f = -N_r(x_{jf} - x_r) + T_r(y_{jf} - y_r) + M_f g(x_{jf} - x_{cmf}) + M_m g(x_{jf}) \quad (4)$$

$$\tau_r = -N_r(x_{jr} - x_r) + T_r(y_{jr} - y_r) + M_f g(x_{jr} - x_{cmr}) \quad (5)$$

The torque required for running the tracks in planar case can be derived from the sum of traction forces at all contact points using (6).

$$\tau_t = (T_f + T_r) D_m / 2 \quad (6)$$

The system has two motors for running the tracks, one each for the left-track and the right-track. Hence, the torque

limits for the front and rear joints and the track are given by (7)

$$|\tau_f|, |\tau_r| \leq \tau_{jmax}, \\ |\tau_t| \leq 2\tau_{tmax} \tag{7}$$

C. Friction constraint

The normal reaction and traction forces at the two contact points should lie within the friction cone. The constraint is given by (8), where μ is the coefficient of friction between the tracks and the terrain which is taken as 0.5. The value of μ was determined experimentally by pully the robot using spring balance and dividing the pulling force by the weight of the robot.

$$|T_f| \leq \mu|N_f|, |T_r| \leq \mu|N_r| \tag{8}$$

D. Geometric constraint

The only geometric constraint is the step height, H_{step}. The difference between Y coordinates of the front contact point and rear contact point is restricted to be equal to the step height in order to meet this constrain as given by (9).

$$y_f - y_r = H_{step} \tag{9}$$

E. Interference avoidance constraint

Constraints need to be defined which prevent solutions resulting in interference between the terrain and the robot. Three types of interferences which can happen are shown in Fig. 5. The constraints which prevent these interferences in the solution are given by (10). The difference between Y coordinates of rear/ front main pulley axes and rear contact point is restricted to be greater than the main pulley diameter. Similarly the difference between Y coordinate of front idler pulley axis and front contact point is restricted to be greater than the idler pulley diameter.

$$y_{jr} - y_r \geq D_m/2, \\ y_{jf} - y_r \geq D_m/2, \\ y_{if} - y_f \geq D_i/2 \tag{10}$$

V. Optimization

The objective function, f, for the optimization problem is joint torque minimization given by (11).

$$f = |\tau_f| + |\tau_r| \tag{11}$$

The design parameters of the optimization problem are $(N_f, T_f, N_r, T_r, \theta_f, \theta_r, \theta_b)$. The front contact point, $(x_f, y_f)_W$ and the step height, H_{step}, are given as inputs for optimization. As shown in Fig. 6. the distance,$D_{contact}$, at which contact is first established with step edge can be determined using (12) for given values of angle of attack, taper angle and step height, H_{step}. The corresponding initial front contact point $(x_{fi}, y_{fi})_W$ is given by (13).

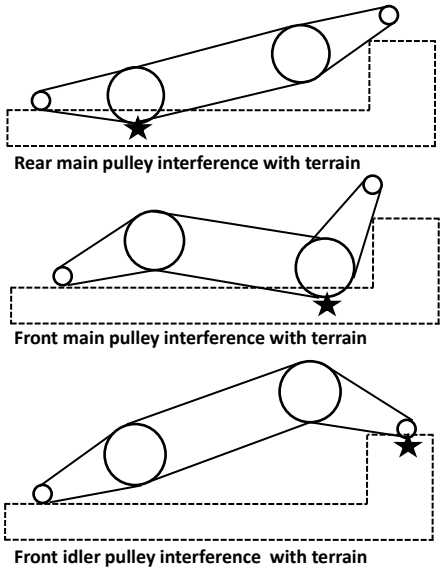

Fig. 5. Three types of possible interference between robot and terrain

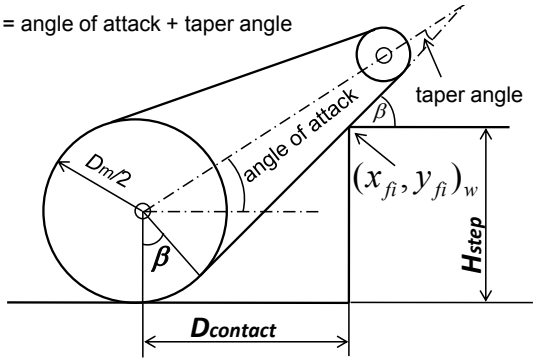

Fig. 6. Initial contact of front segment with step edge

$$D_{contact} = \frac{D_m}{2} sin\beta \\ + \frac{(H_{step} - D_m(1 - cos\beta)/2)}{tan\beta} \tag{12}$$

$$(x_{fi}, y_{fi})_W = (x_{jf}, y_{jf})_W \\ + (D_{contact}, H_{step} - D_m/2) \tag{13}$$

The contact point $(x_f, y_f)_W$ can be anywhere between $(x_{f1}, y_{f1})_W$ and $(x_{f2}, y_{f2})_W$ along the length of the track as shown in Fig. 7. $(x_f, y_f)_W$ is progressively decreased from initial value $(x_{fi}, y_{fi})_W$ to $(x_{f2}, y_{f2})_W$ to emulate the stage-1 of step climbing.

Constraints given by (1), (2), (3), (7), (8), (9), (10) are used for optimization. MATLAB has been used to determine the optimal posture defined by the angles, θ_f and θ_r for given step height and front contact point. The process is repeated keeping the step height constant and decreasing the front contact point from initial value to $(x_{f2}, y_{f2})_W$. This point marks the completion of stage-1 of climbing sequence. The process is repeated for various step heights. Fig. 8 shows the

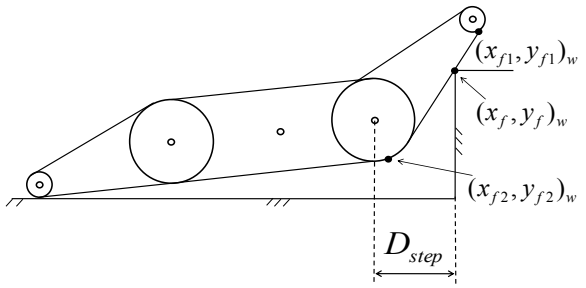

Fig. 7. Range of front contact point location along front track

optimal θ_f and θ_r for angle of attack equal to 70 degrees and step heights of 0.12m, 0.16m, 0.2m, 0.24m, 0.28m and 0.32m as function of the distance, D_{step}. The process is repeated for angle of attack equal to 45 degrees. Fig. 9 shows the optimal θ_f and θ_r for angles of attack equal to 70 degrees and 45 degree for step heights of 0.16m and 0.24m.

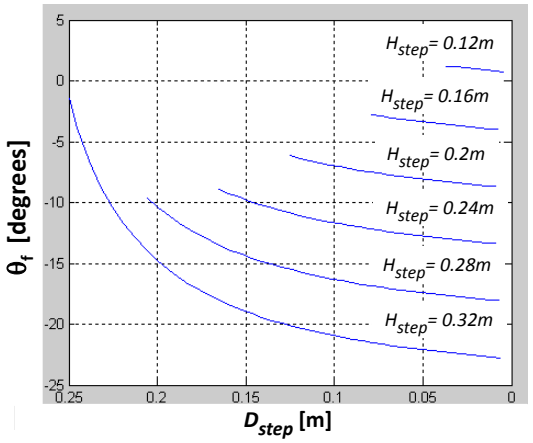

(a)

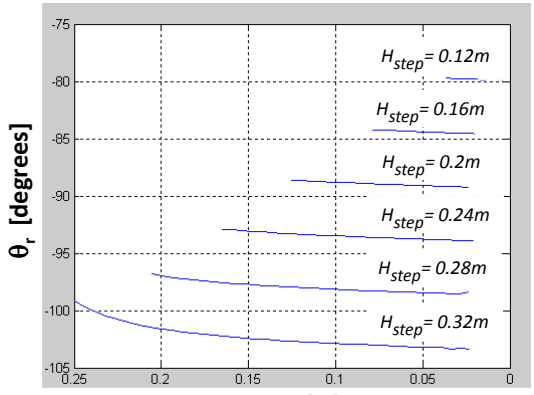

(b)

Fig. 8. Optimum angle of (a) front (b) rear segment as function of distance from step for various step heights

VI. Control Scheme

It can be seen from Fig. 8 that the nature of the curves for θ_f and θ_r is similar for different step heights. However there is a constant offset of 4.7 degrees between the curves.

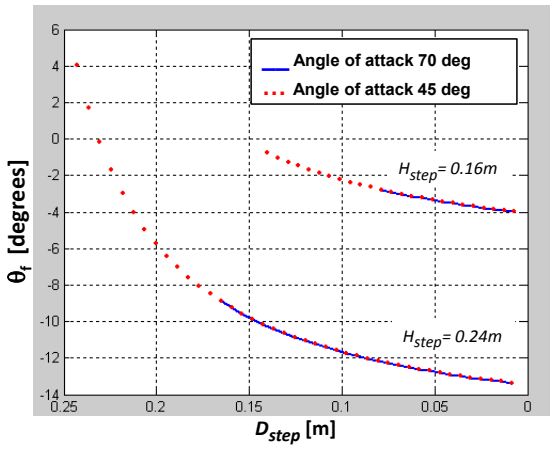

(a)

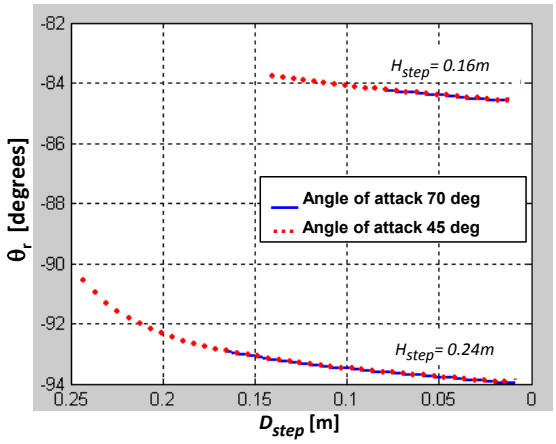

(b)

Fig. 9. Optimum angle of (a) front (b) rear segment as function of distance from step for angle of attack equal to 70 degrees and 45 degrees

This offset, H_{comp}, can be modeled as a linear function of step height, H_{step}. The function was determined empirically and given by (14).

$$H_{comp} = \frac{4.7(0.32 - H_{step})}{0.04} \tag{14}$$

Similarly, it can be concluded from Fig. 9 that the optimum values of θ_f and θ_r are independent of the angle of attack and depend only on the location of the contact point which in turn depends on the step height, H_{step} and the distance D_{step}. It should therefore be possible to approximate the optimum values of θ_f and θ_r by polynomial functions which depend only on the step height, H_{step} and the distance D_{step}. These polynomial functions should work for all permissible step heights and angles of attack.

The values of θ_f and θ_r for step height of 0.32m was fitted against third degree polynomials in the variable D_{step}. The actual values and polynomial approximations of θ_f and θ_r are shown in Fig. 10.

Same polynomials are able to approximate the curves of

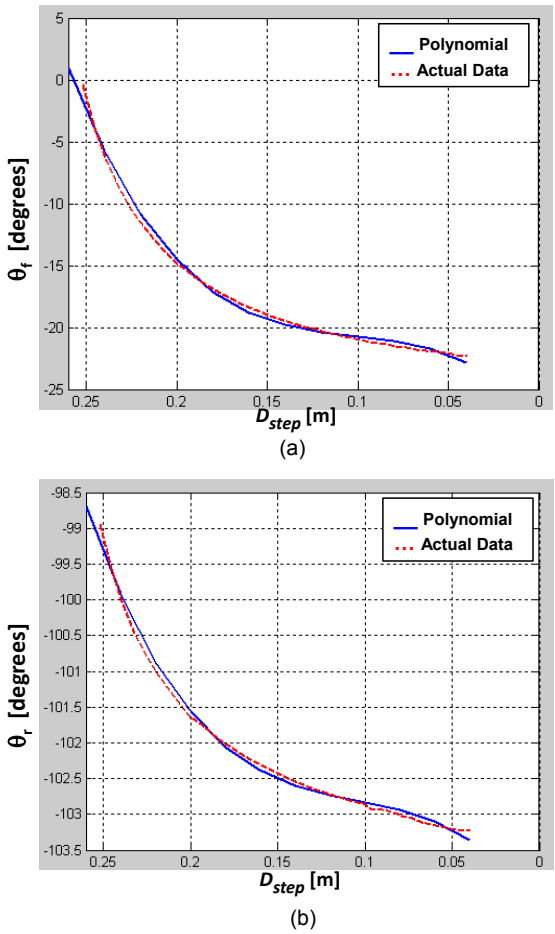

Fig. 10. Actual and polynomial approximation of (a) front (b) rear segment angles as function of distance from step for step height of 0.32m

θ_f and θ_r for different step heights and angles of attack with compensation of H_{comp}. The polynomials approximating the values of θ_f and θ_r are given by (15) and (16) respectively.

$$\theta_f = 4569.7D_{step}^3 - 1355.4D_{step}^2 + 149.3D_{Step} - 26.7 + H_{comp} \quad (15)$$

$$\theta_r = 875.5D_{step}^3 - 271.2D_{step}^2 + 32.75D_{Step} - 104.27 + H_{comp} \quad (16)$$

Angles for the front and rear segments can be calculated using (15) and (16) which are given to the robot to achieve step climbing with minimum torque posture during stage-1. As the distance, D_{step}, reduces to zero the contact point of the robot shifts from the front segment to middle segment marking the beginning of stage-2. The robot is still in minimum torque configuration and same posture can be maintained throughout stage-2. As the robot moves forward the CoM of middle segment crosses the step edge and robot enters stage-3 of climbing. The front and rear segments can be rotated away from the terrain at this stage and the balancing moment results in the whole load supported by middle segment.

VII. Simulation

Using the control scheme described above, simulation was carried out on 3D model of the robot using MSC VISUAL NASTRAN for dynamics simulation and MATLAB SIMULINK for control. The front and rear joint motors are modeled as velocity control rotary actuators. The track motion is emulated by giving surface velocity to the three segments. Step distance and actual angles of the front and rear segments are read from MSC VISUAL NASTRAN by SIMULINK control program. The control program calculates the desired angles of the front and rear segments based on the polynomials (15) and (16). The error in desired and actual values of the angles is used to calculate the velocities of the two joint motors and fed back to the MSC VISUAL NASTRAN model.

A. Step Climbing Simulation

Simulation was carried out for step heights of 0.12m, 0.16m, 0.2m and 0.24m and initial angle of attack equal to 45 degrees. The robot is able to climb steps easily with the posture control scheme. It is found that if the posture control is not implemented the robot is not able to climb at all. However, the real system is able to climb steps due to the presence of cleats along the tracks.

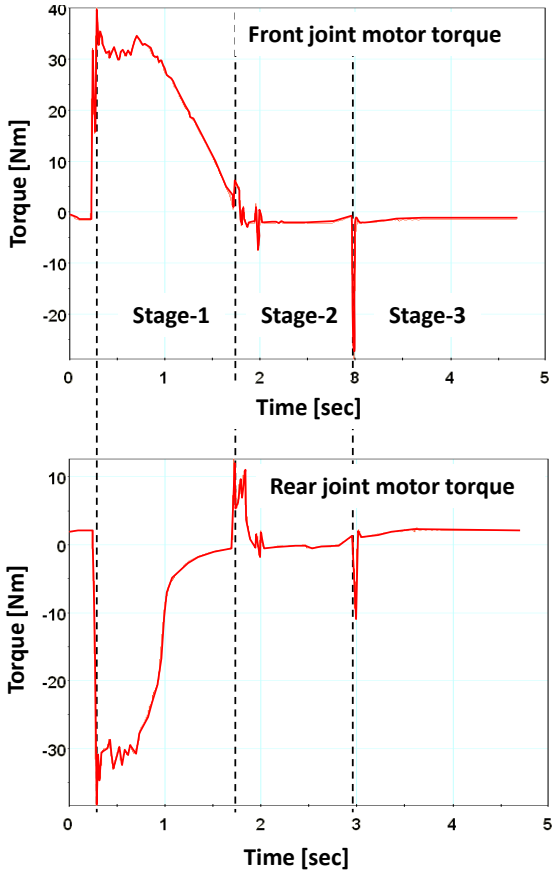

Fig. 11. Torques of front and rear segment motors for step height of 0.240m and angle of attack equal to 45 degrees

The plots of the torques of front and rear segment motor joints during the three stages of climbing are shown in Fig. 11 for step height of 0.24m.It can be seen from the plots of the torques that the magnitude of peak torques is within the maximum limit of motor torques of 35Nm. The torques required during climbing reduce by a factor of ten from beginning to the end of stage-1. Magnitude of the torques required during stage-2 and stage-3 are less than 3 Nm. Snapshots of step climbing sequence during simulation are shown in Fig. 12.

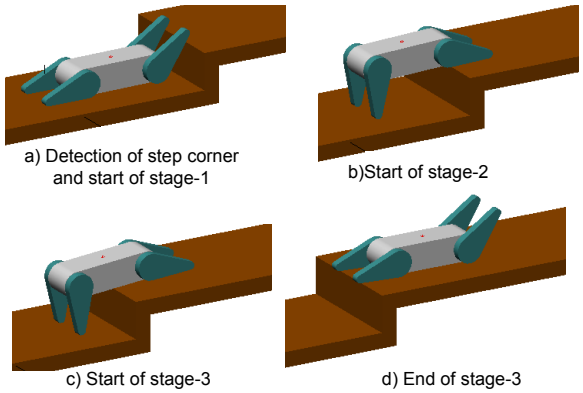

Fig. 12. Snapshots of simulation of step climbing sequence

B. Maximum Step Height Analysis

In order to maximize the step height which the robot can climb the angle of attack can be chosen to make front surface of the front segment parallel to the step. However to ensure a single point of contact with the step edge the angle of attack is kept at 72 degrees resulting in a angle of 5 degrees between the step edge and front segment face as shown in Fig. 13. Step climbing simulation was carried out for different step heights. It was observed that for step height greater than 0.325m the robot completes the stage-1 but topples over before reaching the end of stage-2. This situation arises when the CoM of the middle segment does not cross the step edge and finally results in a moment which topples the robot over. Fig. 14 shows the two situations in which the robot flips to a stable state by end of stage-2 for step height of 0.32m and flip over backwards for step height of 0.33m. The maximum height the robot is able to climb successfully is therefore found to 0.325m.

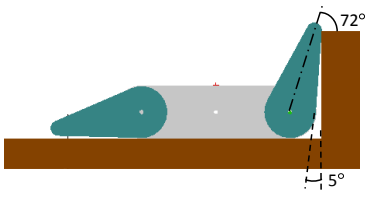

Fig. 13. Configuration with angle of attack equal to 72 degrees

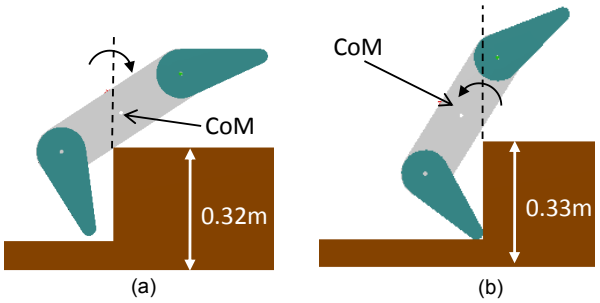

Fig. 14. Configuration at end of stage-2 of climbing (a) Robot flipping towards front for step height 0.32m (b) Robot flipping backwards for step height 0.33m

VIII. Implementation on Real System

Subsequent to verification of the methodology in simulation the algorithm was implemented on the miniUGV. The polynomials for controlling the front and rear joints were implemented in the master controller on the robot. Depending on the height parameter fed through the remote control station via the onboard Linux box and the distance of the step estimated from the speed command for the tracks, the master controller calculates the desired angles and feeds them to the joint controllers in real-time. The joint controllers operating in position control mode achieve the desired angle. In order to measure the total torque applied by the joint motors the motor power was fed from a power supply with current display. The miniUGV was made to climb a step of 0.24m with optimization based algorithm. Fig. 15 gives snapshots of the climbing sequence with optimization implemented. The miniUGV was also made to climb without the optimization by using a fixed posture, similar to the one shown in Start of Stage-1 in Fig. 15, throughout the climbing sequence. Multiple runs of climbing the same step were carried out with and without optimization and the average currents drawn during various stages of climbing were recorded. The average currents drawn during the different stages of climbing in both cases is given in Table III. The standard deviation in the average currents drawn during various runs was found to be within 10%. The overall average current during a climbing sequence is taken as the average of the current during the three stages since the time taken in each stage is approximately equal. It can be seen that there is approximately 30% decrease in average power consumption when using the control scheme presented in this paper.

TABLE III
AVERAGE CURRENT DRAWN DURING DIFFERENT STAGES OF CLIMBING

	STAGE-1	STAGE-2	STAGE-3	Total
With Optimization	3.2A	2A	1.6A	2.26A
Without Optimization	4.7A	3.2A	1.6A	3.2A

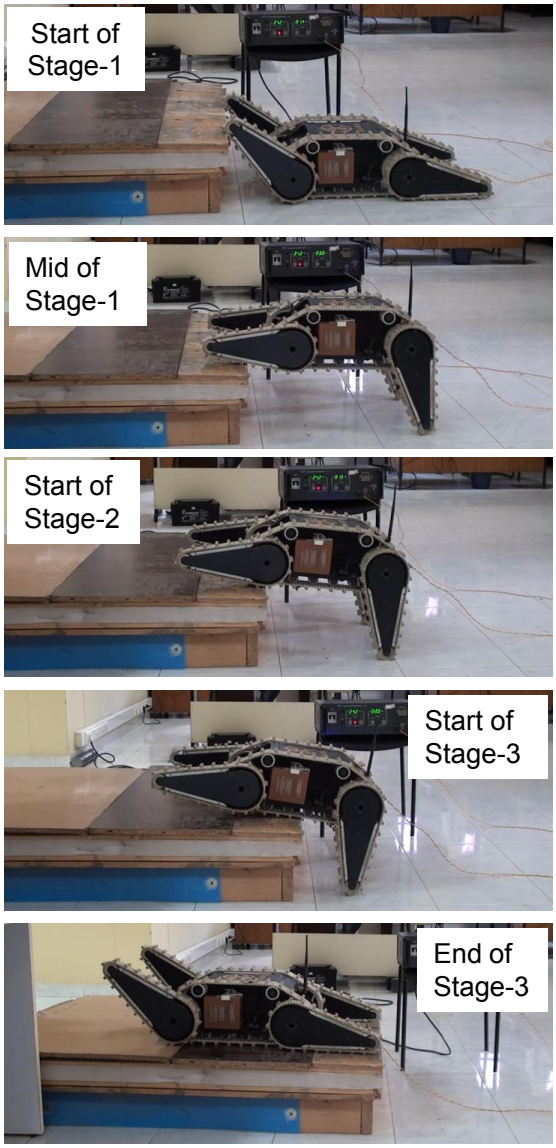

Fig. 15. Snapshots of different stages of the miniUGV climbing step

IX. Conclusion

The posture control methodology developed and presented in this paper, results in torque minimization during step climbing. Implementation of the methodology using polynomials can be easily realized on embedded system to achieve real-time operation. The methodology has been validated on a multi-tracked robot miniUGV resulting in reduction of the total power consumption during step climbing. The methodology has been tested on a simulated step in laboratory conditions. The same will be extended to real world scenarios such as climbing a ledge, debris and footpath as shown in Fig. 16. At present the robot is able to accomplish these without optimization.

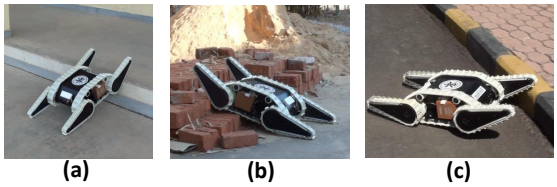

Fig. 16. Snapshots of miniUGV climbing step like features (a) ledge (b) brick pile (c) footpath

Acknowledgement

The authors gratefully acknowledge the Directors of IIIT-Hyderabad and CAIR, DRDO, Bangalore, for their support in carrying out this research.

References

[1] Talon robot. Web page: www.qinetic-na.com/products/unmanned-systems/talon
[2] Matilda robot. Web page: www.mesa-robotics.com/matilda
[3] Packbot from iRobot Corporation, USA. Web page: www.iRobot.com/products_gi
[4] Chaos robot: Web page: www.autonomoussolution.com/chaos-high-mobility-robot.
[5] Weijun Tao, Yi Ou and Hutian Feng "Research on Dynamics and Stability in the Stairs-climbing of a Tracked Mobile Robot" In Proc of the International Journal of Advanced Robotic Systems, 2012.
[6] Homayoun Rastan, "Mechanical Design for Track Robot Climbing Stairs," Masters thesis, Mechanical Engineering, University of Ottawa, July 2011
[7] Nan Li, Shugen Ma, Senior Member, IEEE, Bin Li, Minghui Wang, and Yuechao Wang "An Online Stair-Climbing Control Method for a Transformable Tracked Robot," in IEEE International Conference on Robotics and Automation 2012
[8] Quy-Hung Vu, Byeong-Sang Kim and Jae-Bok Song," Autonomous Stair Climbing Algorithm for a Small Four-Tracked Robot," Korea University.
[9] Suyang Yu, Ting Wang, Yuechao Wang, Di Zhi, Chen Yao, Xiaofan Li, Zhong Wang, and Yu Luo and Zhidong Wang,"A Tip-Over and Slippage Stability Criterion for Stair-Climbing of a Wheelchair Robot with Variable Geometry Single Tracked Mechanism", Proc. of IEEE International Conference on Information and Automation, June 2012
[10] Pinhas Ben-Tzvi, Shingo Ito and Andrew A. Goldenberg., "A mobile robot with autonomous climbing and descending of stairs," In Robotica: page 1 of 18. 2008
[11] Solomon Steplight, Geoffrey Egnal, Sang-Hack Jung, Daniel B. Walker, Camillo J. Taylor and James P. Ostrowski "A Mode-Based Sensor Fusion Approach to Robotic Stair-Climbing" IROS pp. 1113-1118 November 2000.
[12] Anastasios . Mourikis, Nikolas Trawny, Stergios . Roumeliotis, Daniel M. Helmick, and Larry Matthies," Autonomous Stair Climbing for Tracked Vehicles," Proc. of IEEE Internation Journal on Computer Vision 2007.
[13] K. Iagnemma, A. Rzepniewski, S. Dubowsky, and P. Schenker, "Control of robotic vehicles with actively articulated suspensions in roughterrain," Autonomous Robots, vol. 14, no. 1, pp. 516, 2003.
[14] KorhanTurker, Inna Sharf and Michael Trentini, "Step Negotiation with Wheel Traction: A Strategy for a Wheellegged Robot," 2012 IEEE International Conference on Robotics and Automation May 14-18, 2012.
[15] T. Thomson, I. Sharf, B. Beckman, "Kinematic Control and Posture Optimization of a Redundantly Actuated Quadruped Robot," 2012 IEEE International Conference on Robotics and Automation May 14-18, 2012.